Replacing Benzyl Chloride with a Lignin-degradation Product in Cellulose Etherification Decreases the Melting Point

Mohamed Yahia,[a,b] and Ola Sundman [a,*]

A cellulose ether that is easier to melt than benzyl cellulose was produced from the lignin degradation product veratryl alcohol. Veratryl chloride and bromide were synthesized from the alcohol, and these two chemicals were used to react with Avicel® cellulose to form the novel cellulose ether veratryl cellulose (VC). Spectroscopic characterisation techniques (^{1}H NMR, FTIR) indicated the successful conversion of Avicel® cellulose to the cellulose ether VC, by both routes, at a degree of substitution of 1.4 to 1.6. Melting measurements of the VC samples showed a gradual softening from approximately 110 °C; the VC was melted below 200 °C. XRD analysis confirmed that the chemical treatments affect the degree of crystallinity. Size exclusion chromatography results showed that the products differ remarkably in molecular weight. The VC synthesized with veratryl chloride degraded almost twice as much as when veratryl bromide were used. The cellulose ethers were soluble in DMSO, DMAc, and $CHCl_3$.

DOI: 10.15376/biores.18.1.161-174

Keywords: Veratryl cellulose; Melting measurements; Cellulose ether; Degree of substitution; Characterisation techniques; Size exclusion chromatography

Contact information: a: Department of Chemistry, Umeå University, Umeå, SE-90187, Sweden; b: Chemistry Department, Faculty of Science, Helwan University, 11795, Cairo, Egypt;
** Corresponding author: ola.sundman@umu.se*

INTRODUCTION

Although cellulose is a solid and valuable polymer, it has several drawbacks; for example, it is difficult to dissolve and cannot be melted (Lindman *et al*. 2010; Yang *et al*. 2014; Acharya *et al*. 2021). A commonly used strategy to circumvent these problems is to modify the chemical structure of the cellulose, and the products of such chemical modifications are collectively called cellulose derivatives (Zhang *et al*. 2019; Oprea and Voicu 2020; Liu *et al*. 2021; Mali and Sherje 2022).

Cellulose derivatives are divided into two different groups: cellulose esters (*e.g.*, cellulose acetate) and cellulose ethers (*e.g.*, carboxymethyl cellulose) (Candido and Gonçalves 2016). Of these, cellulose ethers are dominating the market, with US$ 11.3 billion in 2021 to $ 14.62 billion in 2016 (Kukoyi 2016). Commercial cellulose ethers are used as thickening, stabilising, water-retaining, and dispersing agents in the building industry (Carraher and Charles 2003; Berglund *et al*. 2009).

The change towards renewable recourses is desirable. However, cellulose etherification is achieved with the use of fossil-based chemicals, *e.g.*, chloroacetic acid and ethyl chloride from fossil sources. The historically important benzyl cellulose (BC) is produced by the etherification of cellulose with petroleum-based benzyl chloride. This

cellulose ether was commercially manufactured before World War II, and it is one of few cellulose derivatives that can display a melting point (Braun and Meuret 1989; Ramos *et al*. 2005). BC is still relevant because it can be used in haemodialysis membranes (Sundman *et al*. 2015), but this polymer is not produced commercially. However, if the fossil-based benzyl chloride (Fig. 1a) could be replaced with a renewable chemical, a fossil-free polymer with similar properties can be produced. If an even more bulky substituent is used, the authors hypothesise that the formed cellulose derivative can show even more mouldable properties than BC.

A structurally related but bulkier chemical is veratryl alcohol (3,4-dimethoxybenzyl alcohol) (Fig. 1b). Veratryl alcohol is a bio-based chemical naturally synthesised from the degradation of lignin. Discovered in 1961 (Russell *et al*. 1961), the biological origin of this lignin-degradation product was established in 1978 (Lundquist and Kirk 1978). The present study used quite strong and toxic chemicals ($SOCl_2$ and PBr_3), but as this is only an initial laboratory study, such processes are not intended for scale-up. For industrial purposes, *e.g.* HCl, a catalyst, high temperature, and pressure, have potential to be used for chlorination.

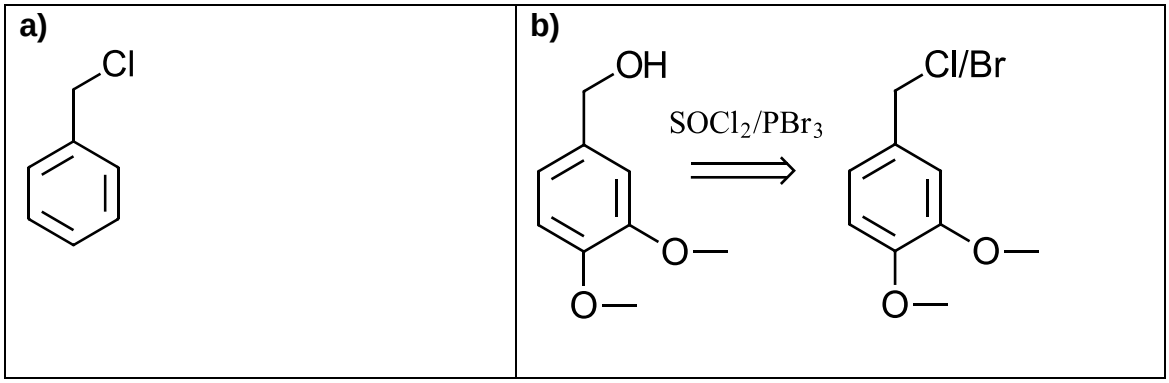

Fig. 1. a) Benzyl chloride, b) Veratryl alcohol (3,4-Dimethoxybenzyl alcohol) to the left and the corresponding chloride/bromide to the right.

As shown in Fig. 1, the difference between benzyl chloride and veratryl chloride is that the latter has two electron-donating methoxy groups. These groups make the veratryl molecules less reactive but more bulky than the respective benzyl group. Thus, a lower melting point can be expected for any veratryl cellulose ether than for the respective benzyl ether.

In this paper, veratryl alcohol was converted to both veratryl chloride and bromide using chemical synthesis, and these products were tested for their reactivity towards cellulose. The produced veratryl cellulose (VC) was characterized using several chemical analyses. According to these principles, a partly bio-based cellulose ether can be synthesised *via* this route, but the veratryl chloride/bromide is probably less reactive than the respective benzyl. The hypothesis is that a cellulose ether that is more easily melted than benzyl cellulose should be formed. The concept presented herein will help develop and synthesise new bio-based cellulose derivatives. Based on this research, decisions can be made to apply this strategy with similar lignocellulose degradation products to further explore the production of different bio-based materials as well as develop cellulose-ether-based bioplastics, *etc*.

EXPERIMENTAL

Materials

Avicel®PH-101 microcrystalline cellulose (~50 µm size, Sigma Aldrich), dimethyl sulfoxide- (DMSO, Sigma Aldrich), trimethylamine (Et_3N, Sigma Aldrich), acetic acid (Sigma Aldich), chloroform ($CHCl_3$, VWR Chemicals), dichloromethane (CH_2Cl_2, VWR Chemicals), phosphorus tribromide (PBr_3, Sigma Aldrich), thionyl chloride ($SOCl_2$, sigma Aldrich), veratryl alcohol (VOH, sigma Aldrich), acetone (Sigma Aldrich), benzyl chloride (Sigma Aldrich), chloroform-D ($CDCl_3$, Armar Chemicals, 99.8 atom%D), dimethyl sulfoxide-d6 (DMSO-d6, Armar Chemicals, 99.8 atom%D), dimethylacetamide (DMAc, VWR Chemicals), 4-dimethylamino pyridine (DMAP, Reagent Plus® ≥99, Sigma Aldrich), methanol (MeOH, VWR Chemicals), propionic anhydride (Sigma Aldrich), 2-propanol (VWR Chemicals), pyridine (Sigma Aldrich), tetrabutylammonium fluoride ($TBAF{\cdot}3H_2O$, Sigma Aldrich), sodium bicarbonate ($NaHCO_3$, VWR Chemicals), anhydrous sodium sulfate (Na_2SO_4, VWR Chemicals), sodium chloride (NaCl, VWR Chemicals) were all used as received. NaOH (VWR Chemicals) was pulverised and used immediately. All the mentioned chemicals were pure (≥ 98%) and used without further purification.

Synthesis of Veratryl Chloride

Following the general procedure in literature (Miyamura *et al*. 2013; Guan *et al*. 2019), 0.60 mL of $SOCl_2$ was added to 1.157 mL of Et3N in an ice bath, and the obtained viscous yellow solution was diluted with 10 mL of dry CH_2Cl_2. The resulting solution was added dropwise to 1.00 mL veratryl alcohol solution in 10 mL of dry CH_2Cl_2. The reaction mixture was allowed to equalise overnight, after which the reaction appeared complete. The reaction mixture was quenched with 10 mL of ice water, stirred for 30 min., and then filtered. The filtrate was dried over anhydrous Na_2SO_4 and then concentrated by rotary evaporation yielding the final product veratryl chloride (3,4-dimethoxybenzyl chloride).

Synthesis of Veratryl Bromide

Following the general procedure in Wu and Huang (2014), veratryl alcohol (9.92 g) was dissolved in 25 mL of CH_2Cl_2, and the solution was cooled to 0 °C. Then, a PBr_3 (1.0 M) solution in CH_2Cl_2 (25 mL) was added via syringe slowly to the alcohol solution. The obtained yellow mixture was stirred at room temperature for another 4 h. The reaction was carefully quenched with ice water (100 mL) and extracted with CH_2Cl_2 (3 x 50 mL). The combined organic layers were successively washed with saturated $NaHCO_3$ (100 mL), distilled water (100 mL), and brine solution (NaCl solution, 100 mL) and dried over anhydrous Na_2SO_4. Finally, the solution was concentrated in a rotary evaporator to collect the desired veratryl bromide (3,4-dimethoxybenzyl bromide).

Synthesis of Benzyl Cellulose (BC) and Veratryl Cellulose (VC)

The synthesis method was based on the procedure reported in the literature (Ramos *et al*. 2005; Sundman *et al*. 2015). Briefly, 2.82 g ($TBAF.3H_2O$) salt was mixed with 15 mL DMSO until fully dissolved; 0.45 g Avicel®PH-101 cellulose was added to the mixture with intense stirring at room temperature (for 30 min) then at 60 °C (for 1 h) until the solution mixture was clear. A solution of (0.37 g pulverised NaOH in 5 mL DMSO) was added to the mixture with vigorous stirring. 1 mL of benzyl chloride was added to the solution with subsequent stirring for 4 h at a constant temperature (70 °C). The produced

benzyl cellulose suspension was precipitated into 1:4 H_2O: MeOH solution and was then neutralised with dilute acetic acid. The benzyl cellulose polymer was obtained by filtration, washing with excess (1:4 H_2O: MeOH) solution, and drying for 48 h under vacuum pressure at 50 °C. The two veratryl cellulose polymers were synthesised similarly but with veratryl chloride or veratryl bromide instead of benzyl chloride and the same molar ratio (1:3) between Avicel cellulose and halide.

Perpropionylation of Avicel® Cellulose And Cellulose Derivatives

Following the synthesis method reported by Sundman *et al*. (2015), a mixture of 0.3 g Avicel® cellulose, 5 mL pyridine, 5 mL propionic anhydride, and 0.2 g DMAP as a catalyst was heated and kept isothermal at 80 °C for >24 h. Then the reaction mixture was cooled to room temperature and precipitated in 200 mL 2-propanol. The obtained polymer was filtered off, washed with 2-propanol, and dried at 70 °C for one week under reduced pressure. The same procedure was used for the perpropionylation of cellulose derivatives by replacing the Avicel® cellulose with the cellulose ethers.

Solubility Measurements

The solubility of the cellulose derivatives was checked by dissolving 10 mg of dry solids in 1 mL solvent. The suspensions were placed in an ultrasonic bath for 30 min, and the samples were visibly swollen. The solubility of the samples was determined visually after resting at room temperature overnight.

Melting Measurements

A few grains of the cellulose ether were transferred to a capillary tube for measurement. The capillaries were put in a melting point apparatus (USA). The samples were heated to 80 °C. The temperature was then gently increased until the material visibly softened, and the temperature was recorded. The temperature was slowly (<10 °C/min) increased to 230 °C with a continuous inspection.

Characterisation Techniques

Nuclear Magnetic Resonances (^{1}H-NMR) spectroscopy was performed to determine the degree of substitution (*DS*) of the cellulose derivatives and recorded using an Avance Bruker DPX (400 MHz). The samples were dissolved in deuterated chloroform solvent, and its ^{1}H-NMR singlet was used as an internal reference ($CDCl_3$, ^{1}H 7.25 ppm).

A Bruker Vertex 80v Fourier Transformed Infrared spectrometer with Attenuated Total Reflectance mode (FTIR-ATR) was used with a detector (deuterated triglycine sulfate-DTGS) to analyse the samples with FTIR. The FTIR spectra range (from 400 to 4000 cm^{-1}) was recorded with 128 scans per sample and a resolution of 4 cm^{-1}.

A size exclusion chromatography (SEC) instrument coupled to a Refractive Index (RI) and a light scattering (LS) detector was used to analyse the molecular weight distribution of the perpropionylated cellulose derivatives. The samples were dissolved in chloroform for measurements at a 5 mg/mL concentration. The SEC system consisted of a high-pressure pump (Hewlett Packard-series 1100), a guard column, two serial T6000M columns, and a 0.45 µm PTFE filter in series. The auto-sampler, columns, and detector temperature were set at 35 °C, the eluent used was chloroform, and the flow rate was 1 mL min^{-1}. The detector system was a Malvern Omnisec Reveal containing a refractive index (IR) and a multi-angle light scattering (MALS) detector. The detector response was calibrated using two polystyrene standards (one broad and one narrow). The data were

evaluated with the Omnisec V11 software from Malvern using the Debye model applying a first-degree polynomial.

X-ray diffractograms (XRD) were obtained using a PANalytical Xpert3 Powder X-ray diffractometer (XRD) with operating system Cu Kα (1.54 Å) radiation at 25 mA and 40 kV. The measurements were recorded from 5° to 45° (2θ) at a scan speed of 8 s per point.

RESULTS AND DISCUSSION

Solubility Test

Table 1 summarises the solubility tests for the cellulose ethers in organic solvents at 25 °C and a concentration of 10 mg/mL. The insolubility of cellulose in common solvents is well-known. The cellulose derivatives were not soluble in hydrogen bonding solvents (MeOH and acetone) but solubilised in the less polar solvents ($CHCl_3$, DMSO and DMAc). Compared to previous literature (Ramos *et al.* 2005, Sundman *et al*. 2015), the solubility here is seen at lower DSs. In both previous studies solubility of BCs was achieved at high DS (>2) and in $CHCl_3$ only. The much higher solubility at more moderate DSs, are indicative of more even distribution of the substutents than in the previous studies (Ramos *et al.* 2005), but the solubility is the only evidence here to support this claim.

Table 1. Solubility of the Cellulose Derivatives in Different Solvents at a Concentration of 10 mg/mL

Sample / Solvent	BC	VC1	VC2
MeOH	i	i	i
$(CH_3)_2O$	i	i	i
$CHCl_3$	s	s	s
DMAc	s	s	s
DMSO	s	s	s

"i" represents insoluble while "s" represents soluble

Melting Measurements

The melting of the BC and the VCs was gradual, and no exact melting point can be reported. In Table 2, the temperatures where first visible softening (FST) of the material could be seen and the temperature where a remarkable change (MST) was observed are reported. It must be stated, however, that the slow and gradual change in structure (softening/melting) can be challenging to exactly determine and that the numbers are based on observations.

Table 2. The First Visible Softening (FST) and the Major Softening Temperature (MST) of the Cellulose Ethers

Name	FST, (°C)	MST, (°C)
BC	107 (3)	137 (6)
VC1	111 (18)	135 (5)
VC2	104 (2)	118 (3)

Average of three to four measurements (standard deviation).

The only observable change was the MST between BC and VC2. However, the softening of these cellulose ethers was gradual, and the melting also depended on impurities in the samples. Interesting, however, is that at even higher temperatures, the VC seemed to melt remarkably. At approximately 170 to 200 °C, both the VCs begun to show a whitish or light-brown melt. The BC did not show any melt; it degraded to a blackish char-like substance, as expected (Isogai *et al*. 1984). These authors showed that the melting of BCs depends on both *DS* and MW and concluded that the *DS* needed to be close to 3 while the degree of polymerisation (*DP*) needed to be < 140 if a clear melting point for BC should appear. The same conclusion cannot be drawn for the VCs studied herein. However, the presence of air bubbles in the samples complicated the interpretation of what is seen in the melting temperature measuring device. It would have been beneficial to perform both the synthesis and the melting measurements in an inert environment to avoid both bubble formation and oxygen catalysed degradation.

Fourier Transform Infrared (FTIR) Measurement

Figure 2 shows the FTIR spectra for the analysed cellulose-based polymers (Avicel® cellulose, BC, VC1, and VC2). The absorption band at (3300 to 3500 cm^{-1}) associated with OH groups (-OH stretching) in cellulose, was diminished and shifted in the spectra for the cellulose ethers (BC, VC1 and VC2). Figure 2 also shows that the absorption band associated with the aromatic rings (C=C stretching mode) appeared around (1450 to 1500 cm^{-1}) for BC and at (1500 to 1600 cm^{-1}) for the VCs, and this increase in wavenumber indicated an increased charge density caused by the donating methoxy groups (Young *et al*. 1951). In the same way, the absorption band associated with aromatic sp2 (C-H bending mode) was shifted. It appeared near 650 to 750 cm^{-1} for BC and around 750 to 850 cm^{-1} for the VCs. Lastly, an absorption band at 1300 to 1250 cm^{-1}, related to the (C–O stretching mode) appeared solely in the VCs due to the methoxy groups in the veratryl structure. In short, the FTIR measurements indicate the successful modification and replacement of OH groups in Avicel® with veratryl groups.

Proton Nuclear Magnetic Resonance (^{1}H NMR) Measurements

The *DS* values of the cellulose ethers were calculated as DS_{NMR} of perpropionylated derivatives, in line with previous work (Ramos *et al*. 2005; Li *et al*. 2011; Sundman *et al*. 2015). DS_{NMR} was estimated according to Eqs. 1 (for P-BC) and 2 (for P-VC1 and P-VC2),

$$DS = \frac{7}{5}\, x\, \frac{A1}{(A2-\frac{2}{5}A1)} \qquad DS = \frac{7}{3}\, x\, \frac{A1}{(A2-\frac{8}{3}A1)} \qquad \text{(1 and 2)}$$

where A1 represents the integral in the ^{1}H NMR spectra for the aromatic peak (δ≈7.2 ppm for P-BC and δ≈6.7 for P-VC1,2), while A2 represents the integration for the aliphatic peaks (the integral of the area $3.0 \leq \delta \geq 5.5$) (Li *et al*. 2011; Ramos *et al*. 2005; Sundman *et al*. 2015). The reasoning behind equations 1 and 2 is found in the supporting information Figs. S1 and S2 (see Appendix). The resulting DS_{NMR} values are presented in Table 3.

Table 3. The DS_{NMR} of the Cellulose (derivatives)

Name	DS_{NMR}
BC	1.2
VC1	1.6
VC2	1.4

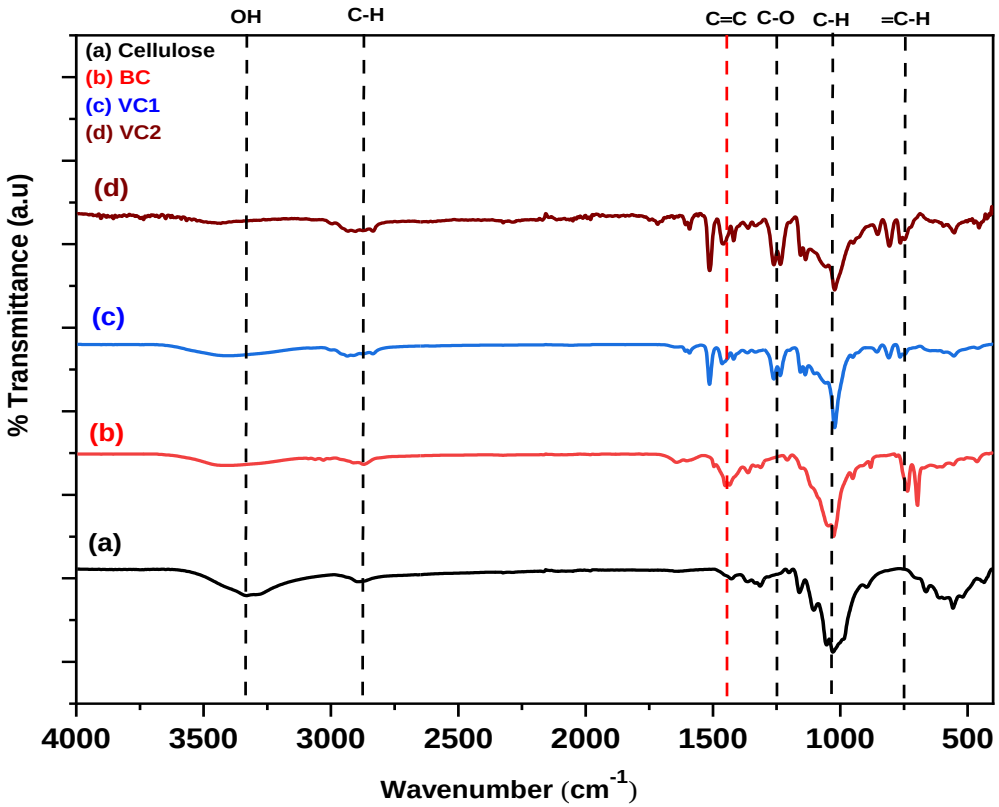

Fig. 2. FTIR spectra of the cellulosic derivatives ((a) Avicel cellulose, (b) BC, (c) VC1, and (d) VC2)

Figure 3a displays (from bottom to top) the ^{1}H NMR spectra of the benzyl chloride (B-Cl), veratryl alcohol - (V-OH), veratryl chloride (V-Cl), and veratryl bromide (V-Br), respectively. The ^{1}H NMR spectrum (400 MHz, internal standard $CDCl_3$) for (B-Cl) showed the two expected signals for benzyl chloride (B-Cl) that appeared at (7.50 ppm, m, 5H) and (4.46 ppm, s, 2H). The ^{1}H NMR spectrum (400 MHz, internal standard DMSO-d6) for veratryl alcohol showed, on the one hand, the five expected peaks appeared for veratryl alcohol (V-OH) at (6.90 ppm, m, 2H), (6.80 ppm, d, 1H), (5.25 ppm, t, 1H), (4.50-4.46 ppm, s, 2H), and (3.85-3.70 ppm, s, 6H). The spectra for veratryl chloride (V-Cl) and veratryl bromide (V-Br) showed all the previously mentioned peaks for (V-OH) except the peak associated with the hydroxyl group. Thus, the ^{1}H NMR analysis indicated the successful synthesis of veratryl chloride or veratryl bromide, respectively, from veratryl alcohol.

The ^{1}H NMR spectra (400 MHz, internal standard $CDCl_3$) of the per-propionylated cellulose derivatives [P-cellulose, P-benzyl cellulose (P-BC) and P-veratryl cellulose (P-VC1 and P-VC2)] are shown in Fig. 3b. The signals for the per-propionylated Avicel® between 3 and 5 ppm were associated with cellulose backbone structure: (H3) 5.10 ppm, (H2) 4.81 ppm, (H1) 4.41 ppm, (H6) 4.06 ppm, (H4) 3.71 ppm, and (H5) 3.53 ppm (Kono *et al*. 2016a; Li *et al*. 2011; Ramos *et al*. 2005). The signals between 0.80 and 2.5 ppm corresponded to the methyl and methylene groups of the propionic acid ester (H7 and H8). In the P-benzyl cellulose (BC) spectrum, it was apparent that additional signals appeared around 7.21 ppm (H9) and 4.65 ppm (H10), which were associated with the benzyl groups (aromatic carbon and methylene groups, respectively).

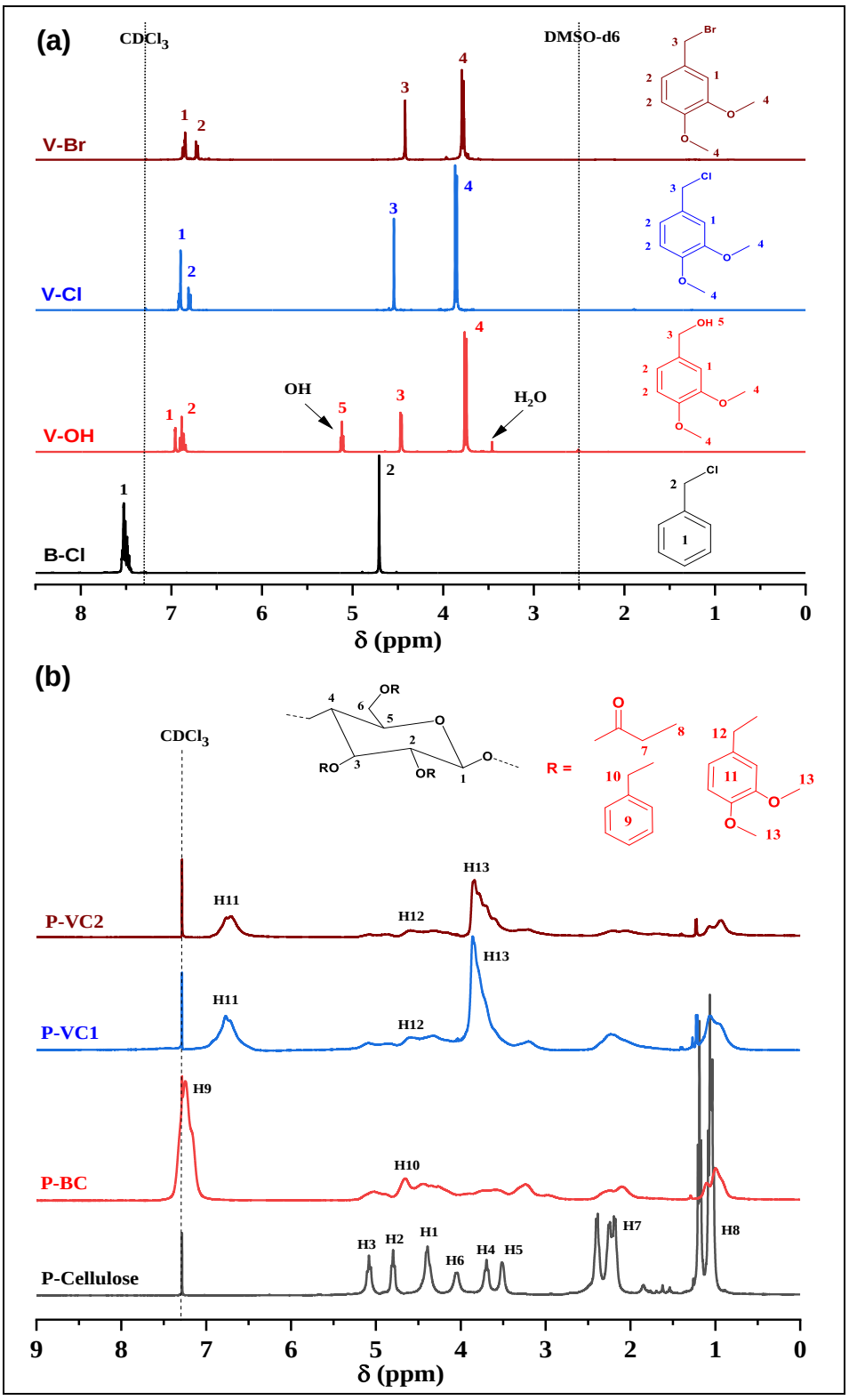

Fig. 3. (a) ^{1}H NMR spectra for (B-Cl), (V-OH), (V-Cl), and (V-Br); (b) ^{1}H NMR spectra for (P-Cellulose), (P-BC), (P-VC1), and (P-VC2).

In the P-veratryl cellulose derivatives (P-VC1 and P-VC2), the corresponding peaks were shifted to around 6.65 ppm (H11), 4.40 ppm (H12), respectively. The reason for the shift between BC and VC structures in the ^{1}H NMR signals was the presence of electron-donating groups (methoxy groups (O-CH_3)) within the veratryl cellulose structures (Spiesecke and Schneider 1961; Kono *et al*. 2016b; Miyamoto and Hada 2021). An additional peak appeared at 3.55 ppm that represents the methoxy group in the veratryl substituents (H13).

Although the ^{1}H NMR spectra were primarily evaluated for DS_{NMR} determination, these data also confirm the successful synthesis of the novel cellulose ether. Overlapping of the cellulose backbone ^{1}H NMR peaks for the ethyl group in benzyl cellulose appeared and the separation of peaks also highly depended on DS_{NMR} (Li *et al*. 2011; Ramos *et al*. 2005). In our data, this phenomenon was also evident in the veratryl cellulose samples. Additionally, as reflected in Table 3, the equal amount of reagent gave higher DS_{NMR} if veratryl chloride (1.6) or bromide (1.4) was used than if benzyl chloride (1.2) was used. However, there is competition between etherification and hydroxide catalysed hydrolysis; hydrolysis might explain the impression of a reversed order of reactivity since it is known to be a quick reaction. However, this is hypothetical, and the molecular weight of the polymers must be considered.

X-ray Diffraction (XRD)

Figure 4 displays the X-ray diffractograms obtained for cellulosic derivatives (Avicel® cellulose, BC, VC1, and VC2).

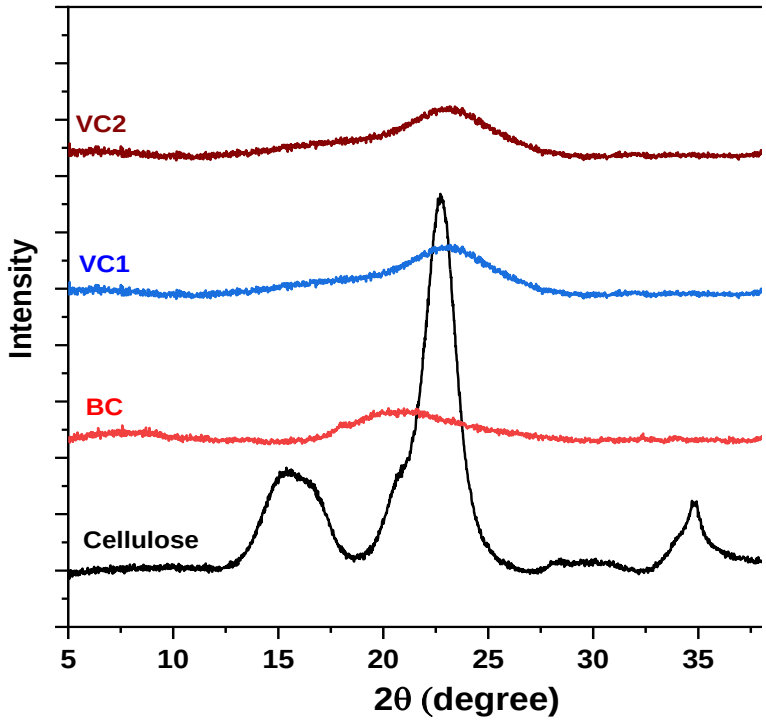

Fig. 4. X-ray diffraction patterns for the cellulosic derivatives (Avicel® cellulose, BC, VC1, and VC2)

The WAXD patterns of Avicel® cellulose showed that there were characteristic diffraction peaks at 2θ = 34.6°, 22.5°, and 16.5°, which correspond to the planes (004), (200) and (110), in Cellulose-I crystals, respectively (Ramos *et al*. 2005; Ass *et al*. 2006; Li *et al*. 2011; Ju *et al*. 2015; Thakur *et al*. 2020). After derivatisation the characteristic peaks of cellulose-I disappeared, and as the degree of crystallisation of cellulosic materials is affected by chemical treatments (Wu *et al*. 2020), the disappearance of crystallinity during the derivatisation process was expected.

Molecular Weight Estimations (Size Exclusion Chromatography)

The SEC analysis was done in chloroform on perpropionylated samples, which all had different molecular weight than the original cellulose (ether). Thus, the molecular weight averages (MW averages: M_w and M_n) had to be calculated with this in mind. Although caution with the SEC of cellulose derivatives as an indication for cellulose molecular weight distribution is advised in the literature (Melander and Vuorinen 2001; Henniges *et al*. 2014; Potthast *et al*. 2015; Li *et al*. 2016; Ono and Isogai 2021), the potential loss of low-MW fractions was not critical. Because only the relative decomposition was analysed, this was not considered an issue. Table 4 displays the MW averages for the original (Avicel®) cellulose and cellulose derivatives (BC, VC1, and VC2), both as data from the SEC measurements and as corrected, calculated using Eq. 3,

$$M_{\mathrm{w,\,corrected}} = M_{\mathrm{w,\,SEC}} * \frac{M_{\mathrm{AGU,non\text{-}per\text{-}propionylated}}}{M_{\mathrm{AGU,per\text{-}propionylated}}} \quad (3)$$

where $M_{\mathrm{w,corrected}}$ represents the corrected, calculated M_w (g/mol) of the polymer in question. $M_{\mathrm{w,\,SEC\,(g/mol)}}$ represents the M_w from the SEC measurement. $M_{\mathrm{AGU,non\text{-}per\text{-}propionylated\,(g/mol)}}$ and $M_{\mathrm{AGU,\,per\text{-}propionylated\,(g/mol)}}$ represent the molecular weight of the AGU of the polymer prior and after per-propionylation, respectively. It was assumed that ($DS_{\mathrm{BC\,or\,VC}}$ + $DS_{\mathrm{per\text{-}propionylation}}$) was 3, which was a simplification. However, any error brought by this simplification was small.

Table 4. Molecular Weight of the AGU (Non-propionylated), Measured and Calculated Molecular Weight Averages, and the Degree of Polymerisation (*DP*) for the Cellulose (Derivatives)

	M (AGU) (g/mol)	M_w (SEC) (g/mol)	M_n (SEC) (g/mol)	M_w (corrected) (g/mol)	M_n (corrected) (g/mol)	DP_w	DP_n
Avicel®	162	80000	46000	40000	22000	240	140
BC	270	56000	37000	41000	27000	150	100
VC1	528	35000	26000	29000	22000	70	60
VC2	488	79000	61000	63000	49000	170	130

The *M* of the AGU of a cellulose derivative depends on both the *DS* of the AGU and the *M* of the substituent. The MW averages of the polymer also depend on the *DP*. VC1 had a higher *DS* for this polymer than both BC and VC2. The *M* of the AGU was also the highest. Nevertheless, the polymer had the lowest MW averages because of the much lower *DP* (*cf.* Table 4), which indicated a considerable degradation. VC2 showed much less degradation. The data indicated more severe degradation during the synthesis of VC1 than VC2. Also, the data indicated almost the same degradation for VC2 as for BC produced with the same amount of reagent and NaOH. The apparent degradation supported

the hypothesis that the competition with alkaline hydrolysis of the cellulose polymer (which is known to happen at these temperatures (Reyes *et al*. 2016)) was responsible for the impression of a reversed order of reactivity towards cellulose: if hydroxide ions were consumed in the substitution reaction, fewer hydroxide ions could depolymerise the cellulose. The less reactive V-Cl consume less OH^- ions, and the opposite would be true; a low polymer *DP* would follow. However, also more V-Cl would remain and the reaction could continue for a long time, thus explaining the DS_{NMR}. Consequently, the reactivity toward Na-cellulose is in the same range for veratryl bromide and benzyl chloride and lower for veratryl chloride. However, the study was brief, and these explanations are not backed by statistics. More experiments are necessary for confirmation.

CONCLUSIONS

1. Veratryl cellulose was found to have excellent solubility and noticeable softening with increased temperature.
2. In these experiments, both veratryl chloride and bromide reacted with cellulose and formed cellulose derivatives with slightly higher *DS* (1.4 to 1.6) than benzyl chloride (1.2) at 1:3 stoichiometric ratio.
3. Veratryl cellulose could be produced as a proof of concept. However, the reactivity of the chemicals could only be understood with both the *DS* values and the *MW averages* in mind. The apparent reactivity of the veratryl bromide was in the same range as benzyl chloride, while the reactivity of veratryl chloride was much lower.

ACKNOWLEDGMENTS

The Kempe Foundations (Sweden) and Bio4Energy, a Strategic Research Environment appointed by the Swedish government, are both acknowledged for supporting this work.

REFERENCES CITED

Acharya, S., Hu, Y., and Abidi, N. (2021). "Cellulose dissolution in ionic liquid under mild conditions: Effect of hydrolysis and temperature," *Fibers* 9(1). DOI: 10.3390/fib9010005

Ass, B. A., Ciacco, G. T., and Frollini, E. (2006). "Cellulose acetates from linters and sisal: Correlation between synthesis conditions in DMAc/LiCl and product properties," *Bioresource Technology* 97(14), 1696-1702. DOI: 10.1016/j.biortech.2005.10.009

Berglund, L., Johansson, K. A., and Sundberg, K. (2009). "Process for the manufacture of methyl cellulose ether," US Patent 7,504,498 B2.

Braun, D., and Meuret, B. (1989). "Benzylcellulose als thermoplastischer Kustoff. I Herstellung und Charactersierung," *Das Papier* 43(12), 688.

Candido, R. G., and Gonçalves, A. R. (2016). "Synthesis of cellulose acetate and carboxymethylcellulose from sugarcane straw," *Carbohydrate Polymers* 152, 679-

686. DOI: 10.1016/j.carbpol.2016.07.071

Carraher, J., and Charles, E. (2003). *Seymour/Carraher's Polymer Chemistry*, CRC Press, Boca Raton, FL, USA.

Guan, L., Zhou, J., Lin, Q., Zhu, H., Liu, W., Liu, B., Zhang, Y., Zhang, J., Gao, J., Feng, F., and Qu, W. (2019). "Design, synthesis and antitumour and anti-angiogenesis evaluation of 22 moscatilin derivatives," *Bioorganic & Medicinal Chemistry* 27(12), 2657-2665. DOI: 10.1016/j.bmc.2019.04.027

Henniges, U., Vejdovszky, P., Siller, M., Jeong, M.-J., Rosenau, T., and Potthast, A. (2014). "Finally dissolved! Activation procedures to dissolve cellulose in DMAc/LiCl prior to size exclusion chromatography analysis–A review," *Current Chromatography* 1(1), 52-68. DOI: 10.2174/2213240601666131118220030

Isogai, A., Ishizu, A., and Nakano, J. (1984). "Preparation of tri-O-benzylcellulose by the use of nonaqueous cellulose solvents," *Journal of Applied Polymer Science* 29(6), 2097-2109. DOI: 10.1002/app.1984.070290617

Ju, X., Bowden, M., Brown, E. E., and Zhang, X. (2015). "An improved X-ray diffraction method for cellulose crystallinity measurement," *Carbohydrate Polymers* 123, 476-481. DOI: 10.1016/j.carbpol.2014.12.071

Kono, H., Oshima, K., Hashimoto, H., Shimizu, Y., and Tajima, K. (2016a). "NMR characterisation of sodium carboxymethyl cellulose 2: Chemical shift assignment and conformation analysis of substituent groups," *Carbohydrate Polymers* 150, 241-249. DOI: 10.1016/j.carbpol.2016.05.003

Kono, H., Oshima, K., Hashimoto, H., Shimizu, Y., and Tajima, K. (2016b). "NMR characterisation of sodium carboxymethyl cellulose: Substituent distribution and mole fraction of monomers in the polymer chains," *Carbohydrate Polymers* 146, 1-9. DOI: 10.1016/j.carbpol.2016.03.021

Kukoyi, A. R. (2016). "Economic impacts of natural polymers," in: *Natural Polymers: Industry Techniques and Applications*, O. Olatunji (ed.), Springer International Publishing, Cham, Switzerland, pp. 339-362. DOI: 10.1007/978-3-319-26414-1_11

Li, M.-F., Sun, S.-N., Xu, F., and Sun, R.-C. (2011). "Cold NaOH/urea aqueous dissolved cellulose for benzylation: Synthesis and characterisation," *European Polymer Journal* 47(9), 1817-1826. DOI: 10.1016/j.eurpolymj.2011.06.013

Li, Y., Shen, H., Lyons, J. W., Sammler, R. L., Brackhagen, M., and Meunier, D. M. (2016). "Size-exclusion chromatography of ultrahigh molecular weight methylcellulose ethers and hydroxypropyl methylcellulose ethers for reliable molecular weight distribution characterisation," *Carbohydrate Polymers* 138, 290-300. DOI: 10.1016/j.carbpol.2015.11.003

Lindman, B., Karlström, G., and Stigsson, L. (2010). "On the mechanism of dissolution of cellulose," *Journal of Molecular Liquids* 156(1), 76-81. DOI: 10.1016/j.molliq.2010.04.016

Liu, K., Du, H., Zheng, T., Liu, H., Zhang, M., Zhang, R., Li, H., Xie, H., Zhang, X., Ma, M., and Si, C. (2021). "Recent advances in cellulose and its derivatives for oilfield applications," *Carbohydrate Polymers* 259, article no. 117740. DOI: 10.1016/j.carbpol.2021.117740

Lundquist, K., and Kirk, T. K. (1978). "De novo synthesis and decomposition of veratryl alcohol by a lignin-degrading basidiomycete," *Phytochemistry* 17(9), 1676. DOI: 10.1016/S0031-9422(00)94674-0

Mali, P., and Sherje, A. P. (2022). "Cellulose nanocrystals: Fundamentals and biomedical applications," *Carbohydrate Polymers* 275, article no. 118668. DOI:

10.1016/j.carbpol.2021.118668
Melander, M., and Vuorinen, T. (2001). "Determination of the degree of polymerisation of carboxymethyl cellulose by size exclusion chromatography," *Carbohydrate Polymers* 46(3), 227-233. DOI: 10.1016/S0144-8617(00)00303-9
Miyamoto, M., and Hada, M. (2021). "^{13}C NMR chemical shifts in substituted benzenes: analysis using natural perturbation orbitals and substitution effects," *Molecular Physics* 119(6), article no. e1843722. DOI: 10.1080/00268976.2020.1843722
Miyamura, H., Choo, G. C. Y., Yasukawa, T., Yoo, W.-J., and Kobayashi, S. (2013). "A heterogeneous layered bifunctional catalyst for the integration of aerobic oxidation and asymmetric C–C bond formation," *Chemical Communications* 49(85), 9917-9919. DOI: 10.1039/C3CC46204H
Ono, Y., and Isogai, A. (2021). "Analysis of celluloses, plant holocelluloses, and wood pulps by size-exclusion chromatography/multi-angle laser-light scattering," *Carbohydrate Polymers* 251, article no. 117045. DOI: 10.1016/j.carbpol.2020.117045
Oprea, M., and Voicu, S. I. (2020). "Recent advances in composites based on cellulose derivatives for biomedical applications," *Carbohydrate Polymers* 247, article no. 116683. DOI: 10.1016/j.carbpol.2020.116683
Potthast, A., Radosta, S., Saake, B., Lebioda, S., Heinze, T., Henniges, U., Isogai, A., Koschella, A., Kosma, P., and Rosenau, T. (2015). "Comparison testing of methods for gel permeation chromatography of cellulose: Coming closer to a standard protocol," *Cellulose* 22(3), 1591-1613. DOI: 10.1007/s10570-015-0586-2
Ramos, L. A., Frollini, E., Koschella, A., and Heinze, T. (2005). "Benzylation of cellulose in the solvent dimethylsulfoxide/tetrabutylammonium fluoride trihydrate," *Cellulose* 12(6), 607-619. DOI: 10.1007/s10570-005-9007-2
Reyes, D. C. A., Skoglund, N., Svedberg, A., Eliasson, B., and Sundman, O. (2016). "The influence of different parameters on the mercerisation of cellulose for viscose production," *Cellulose* 23(2), 1061-1072. DOI: 10.1007/s10570-016-0879-0
Russell, J. D., Henderson, M. E. K., and Farmer, V. C. (1961). "Metabolism of lignin model compounds by *Polystictus versicolor*," *Biochimica et Biophysica Acta* 52(3), 565-570. DOI: 10.1016/0006-3002(61)90415-2
Spiesecke, H., and Schneider, W. G. (1961). "Substituent effects on the C13 and H1 chemical shifts in monosubstituted benzenes," *The Journal of Chemical Physics* 35(2), 731-738. DOI: 10.1063/1.1731993
Sundman, O., Gillgren, T., and Broström, M. (2015). "Homogenous benzylation of cellulose - Impact of different methods on product properties," *Cellulose Chemistry and Technology* 49(9-10), 745-755.
Thakur, M., Sharma, A., Ahlawat, V., Bhattacharya, M., and Goswami, S. (2020). "Process optimisation for the production of cellulose nanocrystals from rice straw derived α-cellulose," *Materials Science for Energy Technologies* 3, 328-334. DOI: 10.1016/j.mset.2019.12.005
Wu, Q., Xu, J., Zhu, S., Kuang, Y., Wang, B., and Gao, W. (2020). "Crystalline stability of cellulose III nanocrystals in the hydrothermal treatment and NaOH solution," *Carbohydrate Polymers* 249, article no. 116827. DOI: 10.1016/j.carbpol.2020.116827
Wu, W.-B., and Huang, J.-M. (2014). "Electrochemical cleavage of aryl ethers promoted by sodium borohydride," *The Journal of Organic Chemistry* 79(21), 10189-10195. DOI: 10.1021/jo5018537
Yang, Y., Xie, H., and Liu, E. (2014). "Acylation of cellulose in reversible ionic liquids," *Green Chemistry* 16(6), 3018-3023. 10.1039/C4GC00199K

Young, C., DuVall, R., and Wright, N. (1951). "Characterisation of benzene ring substitution by infrared spectra," *Analytical Chemistry* 23(5), 709-714. DOI: 10.1021/ac60053a007

Zhang, X., Lin, F., Yuan, Q., Zhu, L., Wang, C., and Yang, S. (2019). "Hydrogen-bonded thin films of cellulose ethers and poly(acrylic acid)," *Carbohydrate Polymers* 215, 58-62. DOI: 10.1016/j.carbpol.2019.03.066

Article submitted: September 26, 2022; Peer review completed: October 22, 2022; Revised version received and accepted: October 27, 2022; Published: November 4, 2022.
DOI: 10.15376/biores.18.1.161-174